arXiv:1112.0851v1 [cond-mat.stat-mech] 5 Dec 2011

Driven Ratchets for Cold Atoms

Ferruccio Renzoni

Departement of Physics and Astronomy, University College London, Gower Street, London WC1E 6BT, United Kingdom

Abstract

Brownian motors, or ratchets, are devices which "rectify" Brownian motion, i.e. they can generate a current of particles out of unbiased fluctuations. The ratchet effect is a very general phenomenon which applies to a wide range of physical systems, and indeed ratchets have been realized with a variety of solid state devices, with optical trap setups as well as with synthetic molecules and granular gases. The present article reviews recent experimental realizations of ac driven ratchets with cold atoms in driven optical lattices. This is quite an unusual system for a Brownian motor as there is no a real thermal bath, and both the periodic potential for the atoms and the fluctuations are determined by laser fields. Such a system allowed us to realize experimentally rocking and gating ratchets, and to precisely investigate the relationship between symmetry and transport in these ratchets, both for the case of periodic and quasiperiodic driving.

Key words: Ratchets, cold atoms, optical lattices
PACS: 05.45.-a, 42.65.Es, 32.80.Pj

Contents

1 Introduction

Brownian motors, or ratchets, are devices which rectify fluctuations, turning in this way unbiased Brownian motion into directed diffusion, in the absence of net applied bias forces.

The concept of ratchet was initially introduced to point out the strict limitations on directed transport at equilibrium imposed by the second principle of thermodynamics (Feynman et al., 1963). Ratchets have then been attracting growing attention in different communities for the number of applications: from particle separation, to the modelling of molecular motors, and to the realization of novel types of electron pumps, just to name a few. Recent reviews (Reimann (2002), Marchesoni and Hänggi (2009)) provide a detailed account of the theoretical work relevant to the ratchet effect, the experimental realizations in many different fields and related practical applications.

The present article reviews recent realizations of driven ratchets for cold atoms. A previous review (Renzoni, 2005) summarized the experimental work at that time. In these cold atom systems, light fields create both a periodic potential for the atoms, and introduce fluctuations in the atomic dynamics. Appropriate ac drivings can also be introduced. The so realized driven ratchets allowed us to experimentally demonstrate many of the characteristic features of ratchets, as for example current reversals. The precise control on the ac drivings also allowed us to investigate from an experimental point of view the relationship between symmetry and transport, which is the essential element for the understanding of the operation of a ratchet.

This review article is organized as follows. In Section 2 the concept of ratchet is introduced, and two early proposals of ratchets discussed: the flashing and

the rocking ratchets. In Section 3 the important role that symmetries play in the operation of a ratchet device is discussed. The symmetry analysis, initially introduced from a general point of view, will then be specialized to a periodically and quasiperiodically driven rocking ratchet, and to a gating ratchet. In Section 4 recent experimental realizations of driven ratchets for cold atoms are reviewed. After introducing the main features of dissipative optical lattices, specific experimental realizations of driven ratchets for cold atoms are examined: a periodically and a quasiperiodically rocking ratchet, and the gating ratchet. Finally, in Sec. 5 possible future directions of research in cold atom ratchets are discussed.

2 Ratchets: generalities

Brownian motors are devices which produce a current out of unbiased fluctuations. Strict limitations on the operation of a ratchet are imposed by the second principle of thermodynamics, which rules out the possibility of producing a current at thermodynamic equilibrium. Thus, the effective generation of a current requires the system to be driven out of equilibrium. We will now examine how this is implemented in two specific cases of ratchet devices: the flashing and the rocking ratchets.

2.1 The flashing ratchet

Consider a sample of Brownian particles in a (static) asymmetric periodic potential. The second principle of thermodynamics rules out the possibility of directed motion. However, things are very different if the potential is "flashed", i.e. if it is turned on and off repeatedly, either periodically or randomly (Ajdari and Prost, 1992; Rousselet et al., 1994). This is sufficient to set the Brownian particles into directed motion, due to the mechanism illustrated in Fig. 1.

Consider an initial situation with the potential turned on and the Brownian particles localized at the bottom of a given well. Then the potential is turned off, and the Brownian particles will symmetrically diffuse in space. Then the potential is turned on again, and the Brownian particles are retrapped in both the original well and in a few neighbouring ones. However, as the potential is asymmetric the retrapping will lead to an asymmetric situation, with the number of particles trapped in the wells at the left of the original well different from the number of particles trapped in the wells at the right of the starting location. Indeed it is clear from Fig. 1 that the wells closer to the "steep wall" of the starting well will collect more particles during the retrapping phase.

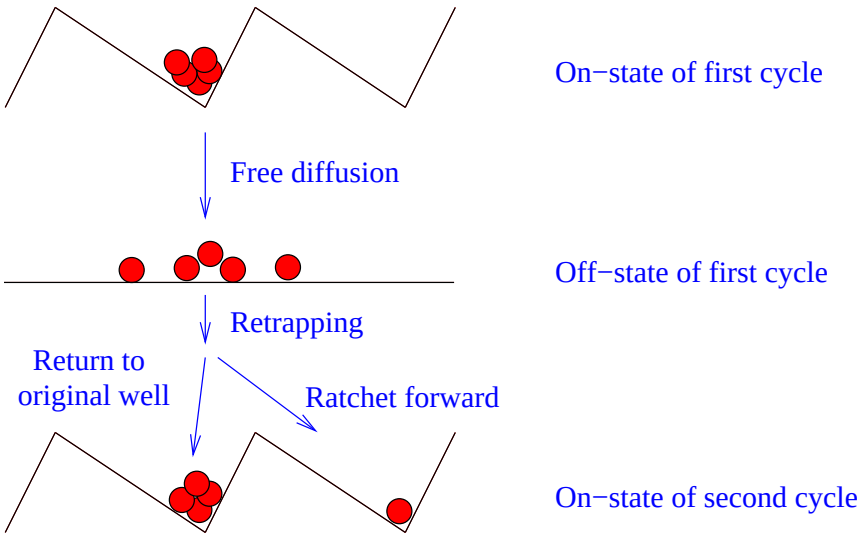

Fig. 1. Working principle of the flashing ratchet.

In this way the center of mass of the particle cloud will move, and directed motion is thus obtained.

It is important to point out why the operation of the flashing ratchet does not violate the second law of thermodynamics. This is because work is done on the system while turning on the potential. Thus, although fluctuations are rectified and a current is generated, this does not imply that work has been extracted out of just one heat source as some additional work was necessary to turn on the potential. Therefore the second law of thermodynamics is not violated.

2.2 The rocking ratchet

In the *rocking* ratchet (Magnasco, 1993; Adjari et al., 1994; Bartussek et al., 1994; Doering et al., 1994), particles in a periodic asymmetric potential experience also an applied ac force. The applied force, which is zero-average and time-symmetric, drives the system out of equilibrium. As a results of the symmetry-breaking anisotropy of the potential, a net current of particles can thus be generated. The same effect can be obtained for a spatially symmetric potential and a temporally asymmetric drive (Mahato and Jayannavar, 1995; Luczka et al., 1995; Chialvo et al., 1996). A bi-harmonic force is a popular choice for a time asymmetric drive, with the time-symmetry of the drive controlled by the relative phase between harmonics (Flach et al., 2000; Yevtushenko et al., 2001; Reimann, 2001; Flach and Denisov, 2004). In the latter case of symmetric potential, and multi-harmonic driving, the underlying rectification mechanism can be traced back to harmonic mixing (Marchesoni, 1986).

Rocking ratchets, and more in general ac driven ratchets, are the central topic of the present review. Therefore, in the following the relationship between symmetry and transport will be examined in detail for these ratchets.

3 Symmetry and transport in ac driven ratchets

The operation of a ratchet requires an out-of-equilibrium set-up, and the breaking of the symmetries which would otherwise prevent directed motion. This Section reviews the symmetry analysis for the specific case of ac driven ratchet, as derived by Flach et al. (2000),Yevtushenko et al. (2001),Reimann (2001),Flach and Denisov (2004).

3.1 General considerations

We consider a Brownian particle in a spatially periodic potential U of period λ. A time-dependent driving force F, of zero mean, is applied to the particle. The Langevin equation for the particle of mass M is:

$$M\ddot{x} + \gamma\dot{x} = -U'(x) + F(t) + \xi(t) \ , \tag{1}$$

where $U'(x)$ denotes the first derivative of the function U. Here x is the position of the particle at the time t, and γ and ξ are the damping coefficient and a stationary Gaussian noise respectively.

Following a standard procedure in the symmetry analysis of ratchet devices (Flach et al., 2000; Yevtushenko et al., 2001; Reimann, 2001; Flach and Denisov, 2004), we aim to determine the conditions for the Langevin equation, Eq. (1), to be invariant under the following symmetries

$$\hat{S}_1 : \ x \to -x + x', \quad t \to t + \tau \tag{2}$$

$$\hat{S}_2 : \ x \to x + \chi, \quad t \to -t + t' \tag{3}$$

with x', t', τ and χ constants. These are the tranformations which map a trajectory $\{x(t, x_0, p_0), p(t, x_0, p_0)\}$, with x_0, p_0 the initial position and momentum, into one with opposite momentum. The invariance of the Langevin equation under $\hat{S}_1$ and/or $\hat{S}_2$ then prevents directed motion.

3.2 The periodically driven rocking ratchet

Whether $\hat{S}_1$, $\hat{S}_2$ are symmetries of the system depends on the specific form of $U(x)$ and $F(t)$. Throughout the present review, we consider only the case of a spatially symmetric periodic potential $U(x+\chi) = U(-x+\chi)$, where χ is a constant. This is the case relevant to the experimental realizations reviewed in this work, with the symmetry of the system controlled by the ac driving. In this Section, we examine the case of a periodic driving $F(t)$, of period T. Following the notations of Flach et al. (2000), we say that $F(t)$ possesses $\hat{F}_s$ symmetry if $F(t)$ is invariant under time reversal, after some appropriate shift:

$$F(t+\tau) = F(-t+\tau) \ . \tag{4}$$

Moreover, if $F(t)$ satisfies:

$$F(t) = -F(t+T/2) \tag{5}$$

we say that F possesses the $\hat{F}_{sh}$ shift-symmetry.

We first consider the dissipationless case, which will then be extended to include weak dissipation.

In the limit of no dissipation, it is immediate to see that if the driving is shift-symmetric then the system is invariant under the transformation $\hat{S}_1$, and current generation is forbidden. If the the driving is symmetric under time reversal, then the system is invariant under the transformation $\hat{S}_2$, and once again directed motion is forbidden.

We now carry further the symmetry analysis for a specific form of driving. We consider the case of a bi-harmonic driving force:

$$F(t) = A\cos(\omega t) + B\cos(2\omega t + \phi) \ . \tag{6}$$

For $A, B \neq 0$ the presence of both an even and an odd harmonic breaks the shift symmetry $\hat{F}_{sh}$, independently of the relative value of the phase ϕ. On the other hand, whether the $\hat{F}_s$ symmetry is broken depends on value of the phase ϕ: for $\phi = n\pi$, with n integer, the symmetry F_s is preserved, while for $\phi \neq n\pi$ it is broken. Therefore for $\phi = n\pi$ current generation is forbidded, while for $\phi \neq n\pi$ it is allowed. Perturbative calculations (Flach et al., 2000) show that the average current of particles is, in leading order, proportional to $\sin\phi$, in agreement with the above symmetry considerations.

We now consider the case of weak, nonzero dissipation. For the sake of simplicity, we restrict our analysis to the case of a bi-harmonic driving of the

form of Eq. (6). As already mentioned the shift-symmetry is broken as the driving consists both of even and odd harmonics. Consider now the symmetry under time-reversal. For $\phi = n\pi$, with n integer, the driving has $\hat{F}_s$ symmetry. However, the system is not symmetric under the transformation $\hat{S}_2$ because of dissipation. Therefore the generation of a current is not prevented, despite the symmetry of the driving. It was shown (Yevtushenko et al., 2001) that the generated current I still shows an approximately sinusoidal dependence on the phase ϕ, but acquires a phase lag ϕ_0: $I \sim \sin(\phi - \phi_0)$. Such a phase lag corresponds to the dissipation-induced symmetry breaking.

3.3 The quasiperiodically driven rocking ratchet

We now consider the case of quasiperiodic driving. We consider a generic driving with two frequencies ω_1, ω_2. Quasiperiodic driving corresponds to an irrational value of the ratio ω_2/ω_1. In order to analyze the relationship between symmetry and transport in the case of a quasiperiodic driving, the two phases

$$\Psi_1 = \omega_1 t \tag{7}$$
$$\Psi_2 = \omega_2 t \tag{8}$$

can be treated as *independent* variables (Neumann and Pikovsky, 2002). The symmetries valid in the case of a perioding driving can then be generalized to the case of a quasiperiodic ac force (Flach and Denisov, 2004).

The driving force $F(t)$ is said to be shift-symmetric, as for the periodic driving case of Sec. 3.2, if it changes sign under one of these transformations:

$$\Psi_i \to \Psi_i + \pi \tag{9}$$

where i is any subset of $\{1, 2\}$, i.e. the π shift is applied to either any of the two variables, of to both of them. If F is shift-symmetric, then the system is invariant under the generalized symmetry

$$\tilde{S}_1 : x \to -x, \quad \Psi_i \to \Psi_i + \pi \tag{10}$$

and directed motion is forbidden.

The driving is said to be symmetric if

$$F(-\Psi_1 + \chi_1, -\Psi_2 + \chi_2) = F(\Psi_1, \Psi_2) \tag{11}$$

with χ_1, χ_2 appropriately chosen constants. If the driving is symmetric, in the dissipationless limit the system is invariant under the generalized symmetry

$$\tilde{S}_2 : x \to x, \quad \Psi_j \to -\Psi_j + \lambda_j \quad (j = 1, 2) \tag{12}$$

and directed transport is forbidden.

The two symmetries are the direct generalization of the symmetries for the periodic case, and control directed motion in the case of a quasiperiodic driving.

3.4 The gating ratchet

In the *gating* ratchet (Savel'ev et al., 2004; Borromeo and Marchesoni, 2005; Borromeo et al., 2006), particles experience an oscillating potential which is spatially symmetric. A zero-average and time-symmetric ac force is also applied. A current can be generated following a gating effect, with the lowering of the potential barriers synchronized with the motion produced by the additive force. This mechanism has to be contrasted with the previously discussed ac-driven ratchets with additive bi-harmonic driving, in which the underlying mechanism is harmonic mixing (Marchesoni, 1986).

The symmetry analysis for the gating ratchet was carried out in Gommers et al. (2008), by following the generale procedure described in Sec. 3.1. Consider a weakly damped particle in an amplitude modulated symmetric potential $V(x)[1 + m(t)]$. A rocking force $F(t)$ is also applied. The Langevin equation for the particle of mass M is:

$$M\ddot{x} + \gamma\dot{x} = -V'(x)[1 + m(t)] + F(t) + \xi(t) \ . \tag{13}$$

Both the amplitude modulation $m(t)$ and the rocking force $F(t)$ are single-harmonic fields:

$$m(t) = m_0 \cos(\omega_1 t) \tag{14}$$
$$F(t) = F_0 \cos(\omega_2 t + \phi) \ . \tag{15}$$

For the symmetry analysis, the noise term $\xi(t)$ can be ignored as it is symmetric. Moreover, the dissipationless limit ($\gamma = 0$) is considered first, and a weak dissipation can be accounted for by an additional phase lag, as discussed previously. The aim of the symmetry analysis is to determine the conditions for the Langevin equation, Eq. (13), to be invariant under the transformations

$\hat{S}_1$, $\hat{S}_2$ (Eqs. 2,3). The invariance of the Langevin equation under $\hat{S}_1$ and/or $\hat{S}_2$ then prevents directed motion.

A relevant quantity for the symmetry analysis is the ratio between the driving frequencies ω_1, ω_2. Limiting ourselves to the case of periodic driving, we express the frequency ratio as $\omega_2/\omega_1 = p/q$, with p, q co-primes. It is straightforward then to show that the Langevin equation is invariant under the transformation $\hat{S}_1$ if q is even. Consider now the invariance under the transformation $\hat{S}_2$. Elementary calculations show that the system is invariant under $\hat{S}_2$ for $q\phi = n\pi$ with n integer, and we therefore expect a current I of the form $I \sim \sin(q\phi)$. The symmetry analysis of Gommers et al. (2008) shows that we should expect no current for q even, and a current of the form $I \sim \sin(q\phi)$ for q odd. These results were obtained in the dissipationless limit. It is straightforward now to take into account the effects of weak dissipation. Dissipation does not affect the reasoning for the symmetry $\hat{S}_1$, i.e we still expect a zero current for q even. On the other hand dissipation breaks the invariance under the time-reversal transformation $\hat{S}_2$, and a current can be generated also for $q\phi = n\pi$. We then expect a current of the form $I \sim \sin(q\phi + \phi_0)$, with the effects of dissipation being accounted for by the phase lag ϕ_0.

4 Cold atom ratchets

The first experiment on the ratchet effect using cold atoms in an optical lattice was reported by Mennerat-Robilliard et al. (1999). In that work directed motion was observed in a spatially asymmetric *undriven* dark optical lattice. The ratchet effect with an undriven optical lattice was later on also demonstrated for the case of spatially symmetric and shifted potentials (Sjolund et al., 2006, 2007; Hagman et al., 2008).

The present work reviews the experimental work on the ratchet effect with *driven* optical lattices. In these experiments ac-drivings are applied, either additively or multiplicatively, to drive the system out of equilibrium and to break the relevant symmetries.

Before entering into the details of the realization of the ac-driven ratchets, we summarize the basics of dissipative optical lattices and the underlying Sisyphus cooling mechanism. We refer to (Grynberg et al., 2001) for a more comprehensive review of optical lattices.

4.1 Dissipative optical lattices

Optical lattices are periodic potentials for atoms created by the interference of two or more laser fields. In near-resonant optical lattices a set of laser fields produce at once the periodic potential acting on the atoms and the cooling mechanism, named Sisyphus cooling, which decreases their kinetic energy. The atoms are finally trapped at the bottom of the potential wells. We describe here the principles of these optical lattices in the case of a one-dimensional configuration and a $J_g = 1/2 \rightarrow J_e = 3/2$ atomic transition. This is the simplest configuration in which Sisyphus cooling takes place.

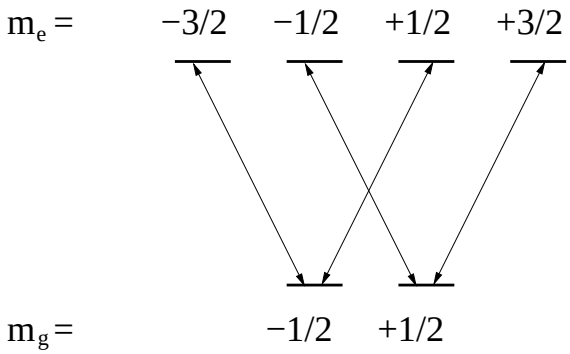

Fig. 2. Atomic level scheme for a $J_g = 1/2 \rightarrow J_e = 3/2$ transition. The arrows indicate the couplings due to σ^+, σ^- laser excitation.

Consider a transition $J_g = 1/2 \rightarrow J_e = 3/2$ (Fig. 2) coupled to two laser fields with the same amplitude and the same wavelength λ, linearly polarized and counterpropagating. These laser fields are detuned below atomic resonance and have orthogonal linear polarization (lin$\perp$lin configuration, see Fig. 3(a)):

$$\vec{E}_1(z,t) = \frac{1}{2}\vec{\epsilon}_x E_0 \exp[i(kz - \omega t)] + c.c \tag{16}$$

$$\vec{E}_2(z,t) = \frac{1}{2}\vec{\epsilon}_y E_0 \exp[i(-kz - \omega t + \alpha)] + c.c \tag{17}$$

where $\vec{\epsilon}_{x,y}$ are the unit vectors of linear polarization along the (x, y) axes and $k = 2\pi/\lambda$ and $\omega = kc$ are the laser field wavevector and angular frequency, respectively. The total electric field is

$$\vec{E}_1(z,t) + \vec{E}_2(z,t) = [E_+(z)\vec{\epsilon}_+ + E_-(z)\vec{\epsilon}_-] \exp(-i\omega t) + c.c. \tag{18}$$

where $\vec{\epsilon}_\pm$ are the unit vectors of circular polarization. After elimination of the relative phase α through an appropriate choice of the origin of the space- and time-coordinates, E_+ and E_- are given by:

$$E_+ = -i\frac{E_0}{\sqrt{2}}\sin kz \ , \tag{19}$$

$$E_- = \frac{E_0}{\sqrt{2}}\cos kz \ . \tag{20}$$

The superposition of the two laser fields E_1, E_2 produces therefore an electric field characterized by a constant intensity and a spatial gradient of polarization ellipticity of period $\lambda/2$, as shown in Fig. 3(a).

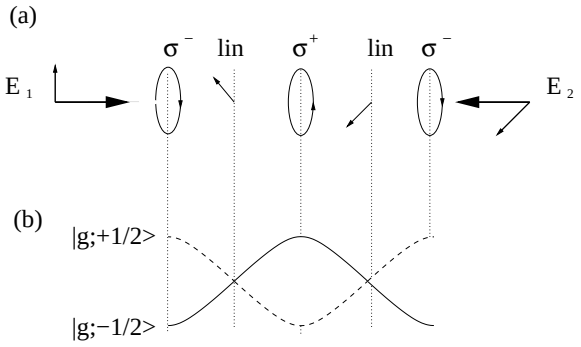

Fig. 3. (a) Arrangement of laser fields in the so-called lin⊥lin configuration, and resulting gradient of ellipticity. (b) Light shift of the two ground-state Zeeman sublevels $|g, \pm 1/2\rangle$.

We examine now the effects that the laser fields have on the atoms. The basic mechanism responsible for the generation of a periodic potential is the "light shift": a laser field coupling a given transition, and characterized by an intensity I_L and detuning Δ from atomic resonance, leads to a shift of the ground state energy ("light shift") proportional to I_L/Δ.

In the present case of a $J_g = 1/2 \rightarrow J_e = 3/2$ transition there are two laser fields coupling each ground state sublevel to the excited state, and contributions from all these couplings have to be taken into account to derive the light shifts $U_\pm$ for the ground state Zeeman sublevels $|g, \pm 1/2\rangle$. We will omit here the details of the calculations, and simply report the final results for the light shifts (see Grynberg et al. (2001) for the derivation):

$$U_+ = 2\hbar\Delta_0' \left(\frac{I_L^+}{I_L} + \frac{I_L^-}{3I_L} \right) \ , \tag{21}$$

$$U_- = 2\hbar\Delta_0' \left(\frac{I_L^-}{I_L} + \frac{I_L^+}{3I_L} \right) \ . \tag{22}$$

Here $I_L^\pm = |E^\pm|^2$ are the intensities of the right- and left-polarization components of the light, and $I_L = I_L^- + I_L^+$ is the total intensity. The quantity Δ_0' is the *light shift per beam* for an optical transition with a Clebsch-Gordan

coefficient equal to 1:

$$\Delta_0' = \Delta \frac{\Omega_R^2/4}{\Delta^2 + \Gamma^2/4}. \tag{23}$$

Here Δ is the detuning of the optical field from atomic resonance and Γ the linewidth of the atomic transition. Ω_R is the Rabi frequency (Cohen-Tannoudji et al., 1998) produced by an electric field of amplitude E_0 driving the optical transition supposing its Clebsch-Gordan coefficient equal to 1. The square of the resonant Rabi frequency is proportional to the light intensity, so in the limit of not too small detuning Δ, we find that the light shift per beam scales as I/Δ, as already mentioned. By substituting the expressions (4.1) for E^+, E^-, the light shifts $U_\pm$ can be rewritten as:

$$U_\pm = \frac{U_0}{2}[-2 \pm \cos kz] \tag{24}$$

with

$$U_0 = -\frac{4}{3}\hbar\Delta_0' \tag{25}$$

the depth of the potential wells. We therefore conclude that the light ellipticity gradient produces a periodic modulation of the light shifts of the ground state Zeeman sublevels (Fig. 3(b)). These periodic modulation acts as an optical potential for the atoms, and indeed these periodically modulated light shifts are usually referred to as *optical potentials*. These optical potentials can be characterized by their depth U_0 or by the related angular vibrational frequency at the bottom of the well ω_v. For a $J_g = 1/2 \rightarrow J_e = 3/2$ atom, the relationship between these two quantities is given by

$$\hbar\omega_v = 2\sqrt{E_r U_0}, \tag{26}$$

where $E_r = \hbar^2 k^2/2M$ is the recoil frequency for an atom of mass M.

We turn now to the analysis of the cooling mechanism, the so-called Sisyphus cooling (Dalibard and Cohen-Tannoudji, 1989), which decreases the kinetic energy of the atoms and allows their trapping at the bottom of the wells of the optical potential.

Sisyphus cooling is determined by the combined action of the light shifts and of optical pumping, which transfers, through cycles of absorption/spontaneous emission, atoms from one ground state sublevel to the other one. This is illustrated in Fig. 4. Consider an atom moving with a positive velocity, and

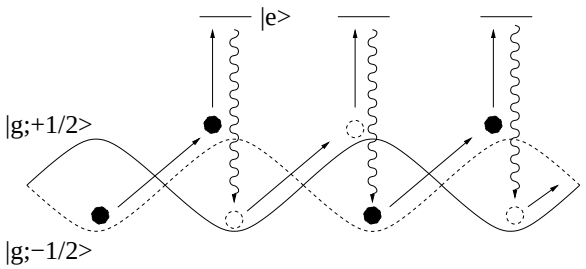

Fig. 4. Sisyphus cooling mechanism.

initially at $z = 0$ in the state $|g, -1/2\rangle$. While moving in the positive z direction the atom climbs the potential curve corresponding to its actual internal state. This has two consequences: first, a part of the kinetic energy of the atoms is transformed in potential energy; second, the component σ^+ of the light increases, which implies the increase of the optical pumping rate towards the level $|g, +1/2\rangle$, i.e. an increase of the probability of transfering the atom from the actual internal state $|g, -1/2\rangle$ to the state $|g, +1/2\rangle$. At the top of the potential hill ($z = \lambda/4$, see Fig. 3) the polarization of the light is purely σ^+, and the probability to transfer the atom into the sublevel $|g, +1/2\rangle$ is very large. The transfer of the atom into the level $|g, +1/2\rangle$ results into a loss of potential energy, which is carried away by the spontaneously emitted photon. This process is repeated several times, until the atom does not have enough energy any more to reach the top of a potential hill, and it is trapped in a well. We notice here the analogy with the myth of Sisyphus, king of Corinth, condemned forever to roll a huge stone up a hill which repeatedly rolls back to the bottom before the summit is reached. This is why the described cooling mechanism has been named Sisyphus cooling. The described cooling process leads to the localization of the atoms at the bottom of the potential wells, and we obtain in this way an *optical lattice*: an ensemble of atoms localized in a periodic potential. We notice that the atoms are localized at the sites where their interaction with the light is maximum. It is because of this property that optical lattices of this type are termed *bright* optical lattices.

An important quantity for the investigations reviewed in this work is the damping rate of the atomic velocity ("cooling rate"). This will be the essential parameter to investigate the phenomenon of dissipation-induced symmetry breaking in a rocking ratchet for cold atoms. Theoretical and experimental work (Raithel et al., 1997; Sanchez-Palencia et al., 2003) showed that the cooling rate is proportional to the scattering rate Γ'. For our 1D configuration and a $J_g = 1/2 \rightarrow J_e = 3/2$ atom, the scattering rate can be expressed as:

$$\Gamma' = \Gamma s_0 = \Gamma \frac{\Omega_R^2/4}{\Delta^2 + \frac{\Gamma^2}{4}} \ , \tag{27}$$

where s_0 is the saturation per beam. Therefore the scattering rate Γ' will be

used in the following to characterize the level of dissipation in the system under consideration.

4.2 Rocking ratchet for cold atoms

The realization of a driven ratchet requires essentially three elements. First, a periodic potential; second, a fluctuating environment which results in friction and in a fluctuating force. Finally, it should be possible to apply a zero-mean ac-force to the particles (the atoms in the present case). All these requirements can be satisfied by using cold atoms in optical lattices, as it was demonstrated by Schiavoni et al. (2003). In that work the one-dimensional spatially symmetric lin⊥lin optical lattice described in Sec. 4.1 was taken as periodic potential.

We turn now to the analysis of the friction and fluctuations in the optical lattice, the second element necessary to use optical lattices as a model system for Brownian motors. As already discussed, the optical pumping between the different atomic ground state sublevels combined with the spatial modulation of the optical potential leads to the cooling of the atoms and to their localization at the minima of the optical potential. The essential fact for the realization of Brownian motors is that even after the cooling phase, characterized by a decrease of the kinetic energy of the atoms and their trapping in the optical potential, the atoms keep interacting with the light fields and this induces fluctuations in the atomic dynamics. Indeed, consider an atom that has already lost enough energy to be trapped at the bottom of a potential well. The atom will then oscillate at the bottom of the well at angular frequency ω_v. This situation is shown in Fig. 5.

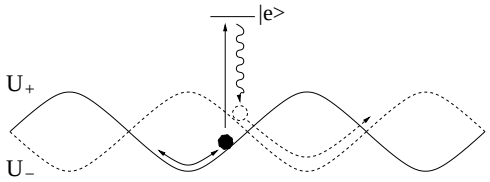

Fig. 5. Stochastic process of optical pumping transferring, via an excited state, an atom from a potential to the other one. The filled (empty) circle represents the atom in the $|g, +1/2\rangle$ ($|g, -1/2\rangle$) ground state sublevel.

To be specific, consider for example an atom initially in the $|g, +1/2\rangle$ state. Exactly at the center of the well the light polarization is purely σ^+, which does not allow the transfer from the $|g, +1/2\rangle$ state to the $|g, -1/2\rangle$ sublevel. However, out of the center of the well the light has also a nonzero σ^- component, which results in a nonzero probability to transfer the atom from its original sublevel to the other one. Therefore the atom can be transfered from one sublevel to the other one, and also the potential experienced by the atom will change from U_+ to U_-, i.e. the force experienced by the atom will change.

As optical pumping is a stochastic process, the (stochastic) transfer from a sublevel to the other one results in a *fluctuating force*. Figure 5 also shows how optical pumping between different optical potentials leads to the transport of atoms through the lattice: although the trapped atom does not have enough energy to climb the potential hill, optical pumping allows the transfer from a potential well to the neighbouring one. The optical pumping leads then to a *random walk* of the atoms through the optical potential, and indeed normal diffusion has been experimentally observed for an atomic cloud expanding in an optical lattice (Carminati et al., 2001).

Two different quantities, the diffusion coefficients in momentum space D_p and in real space D_{sp}, can be introduced to characterize the atomic random walk in momentum and position respectively.

The momentum diffusion coefficient D_p, as determined by the fluctuations in the dipole force, scales as U_0^2/Γ' (Dalibard and Cohen-Tannoudji, 1989). The fluctuations in the dipole force are the main heating process in Sisyphus cooling. Thus the momentum diffusion coefficient determines, via the Einstein relation $k_B T = D_p/\gamma$ with γ the friction coefficient, the equilibrium temperature, which is found to be proportional to the potential depth U_0 (Dalibard and Cohen-Tannoudji, 1989).

The spatial diffusion coefficient D_{sp} is instead predicted to be, for the range of lattice parameters corresponding to normal diffusion, approximately proportional to the scattering rate Γ' (Grynberg et al., 2001).

The last element necessary to implement a rocking ratchet is the oscillating force. In order to generate a time-dependent homogeneous force, one of the lattice beams is phase modulated, so to obtain the electric field configuration:

$$\frac{1}{2}E_0 \left\{\vec{\epsilon}_x \exp[i(kz - \omega t)] + \vec{\epsilon}_y E_0 \exp[i(-kz - \omega t + \alpha(t))]\right\} + c.c. \ , \qquad (28)$$

where $\alpha(t)$ is the time-dependent phase. In the laboratory reference frame this laser configuration generates a moving optical potential $U[2kz - \alpha(t)]$. Consider now the dynamics in the moving reference frame defined by $z' = z - \alpha(t)/2k$. In this accelerated reference frame the optical potential is stationary. In addition to the potential the atom, of mass m, experiences also an inertial force F in the z direction proportional to the acceleration a of the moving frame:

$$F = -Ma = \frac{M}{2k}\ddot{\alpha}(t) \ . \qquad (29)$$

In this way in the accelerated frame of the optical potential the atoms experience an homogeneous force which can be controlled by varying the phase $\alpha(t)$ of one of the lattice beams.

The appropriate choice of the phase $\alpha(t)$ for the realization of the spatially symmetric rocking ratchet is

$$\alpha(t) = \alpha_0 \left[\cos(\omega t) + \frac{\alpha_2}{4}\cos(2\omega t - \phi)\right] \tag{30}$$

with ϕ constant. Indeed, by using Eq. (29), we can see immediately that in the accelerated frame of the optical potential the phase modulation $\alpha(t)$ will result into a force

$$F = \frac{M\omega^2\alpha_0}{2k}\left[\cos(\omega t) + \alpha_2\cos(2\omega t - \phi)\right] \tag{31}$$

with α_2 the relative weight of the 2ω term. This force is of the form needed for the realization of the spatially symmetric rocking ratchet.

Experimentally, it is possible to obtain a phase modulation of the form (30) by simply using acousto-optical modulators and a set of radio-frequency generators. The exact technical realization is of no particular interest here, and we refer to Schiavoni et al. (2003) for further details. We only notice that it is possible experimentally to carefully control the phase difference ϕ between the two harmonics. This allows us to carefully control the symmetry of the system.

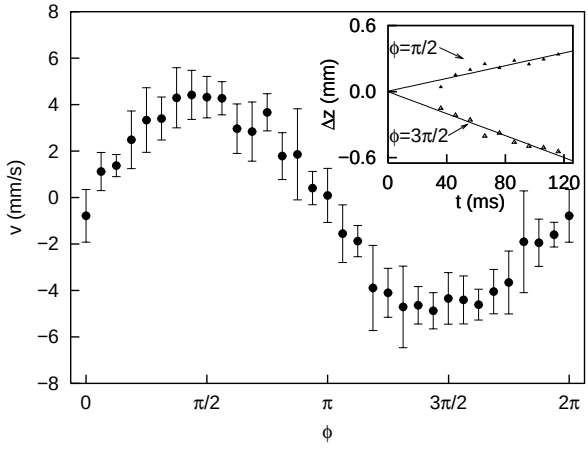

Fig. 6. Average atomic velocity as a function of the phase ϕ. Inset: displacement of the center of mass of the atomic cloud as a function of time for two different values of the phase ϕ. [Reprinted figure with permission from Schiavoni et al. (2003). Copyright 2003 of the American Physical Society.]

The experiment of Schiavoni et al. (2003) on ^{85}Rb atoms clearly demonstrated the control of the current through a spatially symmetric potential by varying

the time-symmetries of the system. In that work, the dynamics of the atoms in the optical lattice was studied by direct imaging of the atomic cloud with a CCD camera. For a given phase ϕ the position of the center of mass of the atomic cloud was studied as a function of time. It should be noticed that in principle it is necessary to transform the measurements from the laboratory reference frame to the accelerated reference frame of the optical potential, by using the coordinate transformation $z' = z - \alpha(t)/2k$. However in the case of Schiavoni et al. (2003) this is not necessary as for the typical time scales of that experiment (period of the ac force and imaging time) the measured positions of the c.m. of the atomic cloud in the laboratory and in the accelerated reference frame are approximately equal. The results of that experiment are reported in Fig. 6. It can be seen that the center of mass of the atomic cloud moves with constant velocity (see inset). This velocity shows the expected dependence on the phase ϕ: for $\phi = n\pi$, with n integer, the velocity (current of atoms) is zero, while for $\phi = \pi/2, 3\pi/2$ the velocity reaches a maximum (positive or negative). This because although the symmetry $F(t+T/2) = -F(t)$ is broken for any value of the phase ϕ, there is a residual symmetry $F(t) = F(-t)$ which forbids the current generation. This symmetry is controlled by the phase ϕ: for $\phi = n\pi$ it is realized, while for $\phi = (2n+1)\pi/2$ it is maximally broken.

The experiment of Schiavoni et al. (2003) proved that the atoms can be set into directed motion through a symmetric potential by breaking the temporal symmetry of the system. That described experiment reproduced well the dependence of the current on the phase ϕ derived in Sec. 3.2 on the basis of the analysis of symmetries which apply in the Hamiltonian limit, i.e. in the absence of dissipation. This because Schiavoni et al. (2003) performed the experiment in the regime of relatively strong driving and small damping, which well approximates the Hamiltonian regime, as confirmed by detailed numerical simulations (Brown and Renzoni, 2008).

4.3.1 Dissipation-induced symmetry breaking

As discussed in Sec. 3.2, the presence of weak damping results in a shift of the curve representing the current as a function of the relative phase between the driving harmonics. This corresponds to a dissipation-induced symmetry breaking, with the generation of a current for a system Hamiltonian symmetric in time and space. Such a ratchet regime was demonstrated experimentally by Gommers et al. (2005b).

In that experiment cesium atoms were loaded in a 3D optical lattice. A bichromatic driving force along one direction was applied by phase-modulating one of the lattice beam. A rocking ratchet was realized in this way. The level of dissipation was quantitatively characterized by the photon scattering rate Γ', which can be controlled experimentally by varying the lattice fields parame-

ters.

Different sets of measurements were performed for different values of the scattering rate Γ' at a constant depth of the optical potential. This was done by varying simultanously the intensity I_L and detuning Δ of the lattice beams, so to keep the potential depth $U_0 \propto I_L/\Delta$ constant while varying the scattering rate $\Gamma' \propto I_L/\Delta^2$. We notice that as I_L and Δ can be varied only within a finite range, dissipation cannot be suppressed completely, i.e. it is not possible to obtain $\Gamma' = 0$. However, as we will see, for the driving strength considered in the experiment, the smallest accessible scattering rate results in a phase shift which is zero within the experimental error, i.e. this choice of parameters well approximates the dissipationless case. By then increasing Γ' it was possible to investigate the effects of dissipation.

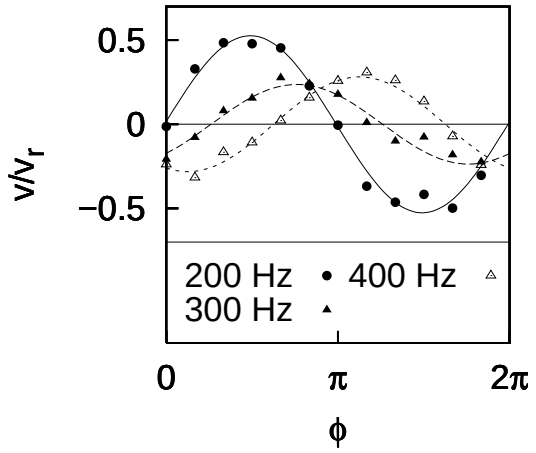

Fig. 7. Experimental results for the average atomic velocity, in units of the recoil velocity $v_r = \hbar k/M$, as a function of the phase ϕ. The recoil velocity is equal to 3.52 mm/s for the D_2 line of Cs atoms. The lines are the best fit of the data with the function $v = v_{max} \sin(\phi - \phi_0)$. The optical potential is the same for all measurements, and corresponds to a vibrational frequency $\omega_v/(2\pi) = 170$ kHz. Different data sets correspond to different scattering rates obtained by varying the lattice detuning Δ and keeping constant the potential depth. The data are labeled by the quantity $\Gamma_s = [\omega_v/(2\pi)]^2/(\Delta/(2\pi))$ proportional to the scattering rate, reported in the bottom part. Driving parameters of the driving are $\omega/(2\pi) = 100$ kHz, $\alpha_0 = 27.2$rad, $\alpha_2 = 4$. [Reprinted figure with permission from Gommers et al. (2005b). Copyright 2005 of the American Physical Society.]

The results of the measurements of Gommers et al. (2005b), reported in Fig. 7, demonstrate clearly the phenomenon of dissipation-induced symmetry-breaking. In agreement with previous theoretical work (Flach et al., 2000; Yevtushenko et al., 2001), the measured current of atoms is well approximated by $I_{max} \sin(\phi - \phi_0)$. Therefore, by fitting data as those reported in Fig. 7 with the function $v = v_{max} \sin(\phi - \phi_0)$ the phase shift ϕ_0 was determined as a function of Γ', as reported in Fig. 8. The measured phase shift ϕ_0 is zero, within the experi-

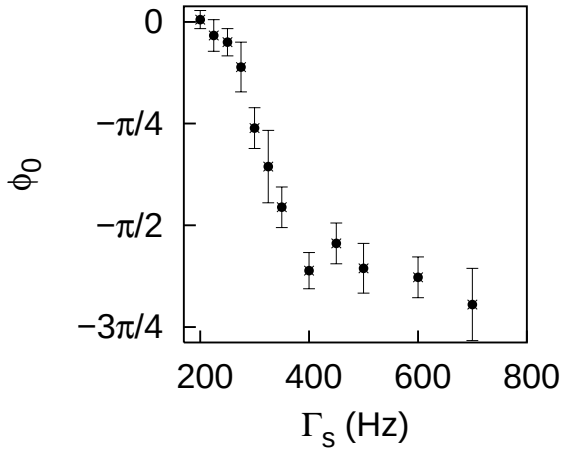

Fig. 8. Experimental results for the phase shift ϕ_0 as a function of $\Gamma_s = [\omega_v/(2\pi)]^2/(\Delta/(2\pi)$, which is proportional to the scattering rate. All the other parameters are kept constant, and are the same as for Fig. 8. [Reprinted figure with permission from Gommers et al. (2005b). Copyright 2005 of the American Physical Society.]

mental error, for the smallest scattering rate examined in the experiment. In this case, no current is generated for $\phi = n\pi$, with n integer, as for this value of the phase the system is invariant under time-reversal transformation. The magnitude of the phase shift ϕ_0 increases at increasing scattering rate, and differs significantly from zero. The nonzero phase shift corresponds to current generation for $\phi = n\pi$, i.e. when the system Hamiltonian is invariant under the time-reversal transformation. This result clearly demonstrates the breaking of the system symmetry by dissipation.

4.3.2 Rectification of fluctuations, current reversals and resonant activation in a system with broken Hamiltonian symmetry

The cold atom experiments reviewed so far aimed to investigate the relationship between symmetry and transport in rocking ratchets. In those experiments the generation of a current was studied as a function of the parameters controlling the symmetry of the system: the relative phase ϕ, which controls the symmetry of the driving, and the scattering rate, which controls the symmetry-breaking of the system by dissipation.

However, in many other ratchet experiments, different aspects of ratchets are investigated. Instead of studying the current as a function of the symmetry-breaking parameters, a given investigation considers thoroughly a system with broken Hamiltonian symmetry. This can be realized, for example, by using a rocking ratchet with a spatially asymmetric potential or a temporally asymmetric force. That study of the ratchet current amplitude as a function of the system parameters (driving amplitude and frequency, noise strength) reveals

several distinguishing features of the ratchet effect. Namely, current reversals are observed in correspondence of the variation of the driving amplitude and frequency. Furtermore, a non-monotonic dependence of the amplitude of the generated current on the fluctuations level is a signature of the rectification of fluctuations associated with the ratchet process.

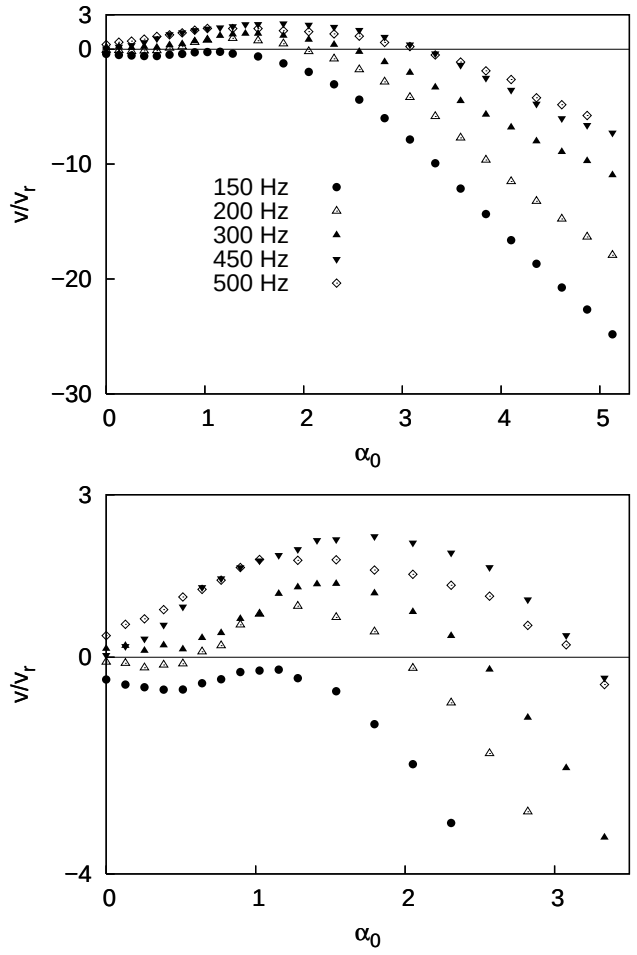

Fig. 9. Experimental results for the atomic velocity as a function of the amplitude of the phase modulation. The relative weight of the 2ω term of the modulation (see Eq. 30) is $\alpha_2 = 1$ for all data sets. The top graph include all experimental results, while the bottom graph evidences the region of small ac forces. The optical potential is the same for all measurements. Different data sets correspond to different optical pumping rate, and they are labeled by $\Gamma_s = [\omega_v/(2\pi)^2]/(\Delta/(2\pi))$ (ω_v is the vibrational frequency) which is proportional to the optical pumping rate. [Reprinted figure with permission from Jones et al. (2004). Copyright 2004 of the American Physical Society.]

Investigations along these lines with cold atom ratchets with broken Hamiltonian symmetry led to the observation of several hallmarks of the ratchet effects. In the experiments by Jones et al. (2004) and Gommers et al. (2005a), a

spatially symmetric rocking ratchet with bi-harmonic driving was considered. Throughout those investigations, the relative phase between the harmonics of the driving was fixed to $\phi = \pi/2$, so that the Hamiltonian time-symmetry of the system was broken.

In Jones et al. (2004) the current of atoms through the lattice was studied as a function of the strength of the applied ac force for different values of the optical pumping rate Γ'. Results of those measurements, reported in Fig. 9, show a clear dependence of the atomic current on the amplitude of the applied force and on the optical pumping rate. Consider first the dependence on the ac force magnitude. For a small amplitude of the ac force the average atomic velocity is an increasing function of the force amplitude, with the atoms moving in the positive direction. At larger amplitude of the ac force the velocity decreases, and a current reversal is observed, with the atomic cloud moving in the negative direction. This kind of behaviour, named *current reversal*, is a hallmark of rocking ratchets. We examine now the dependence of the current on the optical pumping rate, i.e. on the noise level. We observe from Fig. 9 that such a dependence is very different depending on the ac force amplitude. For large amplitude of the applied force the magnitude of the current (in absolute value) is a decreasing function of the optical pumping rate. This means that in this regime the motion can be attributed to deterministic forces and correspond to force rectification by harmonic mixing: in a nonlinear medium the two harmonics, of frequency ω and 2ω and phase difference ϕ, are mixed and the rectified force produces a current $I \sim \sin\phi$. In the considered experiment the nonlinearity of the medium is the anharmonicity of the optical potential. In this regime of rectification of the forces the noise does not play any constructive role in the generation of the current of atoms. On the contrary, the noise disturbs the process of rectification of the forces, and indeed the current decreases for increasing optical pumping rate. Thus, this regime does not correspond to the rectification of fluctuations. A very different dependence of the current amplitude on the optical pumping rate was found in the regime of small amplitudes of the applied force. Indeed in this regime the current is for small pumping rates an increasing function of the pumping rate, and the current vanishes in the limit of vanishing optical pumping rates. At larger pumping rates the current reaches a maximum and then decreases again. This bell-shaped dependence of the current on the optical pumping rate is a typical signature of a Brownian motor: in the absence of fluctuations the current is zero, then increases until the fluctuations are so large that the presence of the potential and of the applied fields become irrelevant, and the current decreases again. Thus, in the regime of small ac force amplitude the optical lattice provides an implementation of a Brownian motor.

Another important parameter for the rectification mechanism is the driving frequency. Consider first the problem of the escape of a Brownian particle from a *single* potential well. It is well known that in the presence of nonadi-

abatic driving the lifetime of the particle in the well can be significantly reduced, a phenomenon named *resonant activation* (Devoret et al., 1984, 1987; Dykman et al., 2001). Resonant activation has also been theoretically studied for Brownian particles in periodic potentials. Also in this case the nonadiabatic driving may result in a significant enhancement of the activation rate. Moreover, whenever the spatio-temporal symmetry of the system is broken, the resonant activation gives then rise to *resonant* rectification of fluctuations (Dykman et al., 1997; Goychuk and Hänggi, 1998; Luchinsky et al., 2000). The resonant activation results in a resonance as function of the driving frequency in the current of atoms through the periodic potential. The theoretical work (Dykman et al., 1997; Soskin et al, 2003; Luchinsky et al., 2000) also predicted that by changing the frequency of the driving it is possible to control the direction of the diffusion.

The experimental work by Gommers et al. (2005a) precisely studied the driving frequency dependence of the rectification mechanism in a periodically driven rocking ratchet for cold atoms. In that work, the current of atoms through the ac driven lattice was studied as a function of the driving frequency ω, for a given relative phase $\phi = \pi/2$ between the driving harmonics, so to break the time-symmetry of the system. The build-up of a resonance was observed when the amplitude of the driving was progressively increased, as shown in Fig 10. The resonance appears in the regime of non-adiabatic driving ($2\omega \gtrsim \omega_v$), and a current reversal is observed on the low-frequency side of the resonance, in agreement with the general theory (Dykman et al., 1997; Soskin et al, 2003; Luchinsky et al., 2000).

4.4 Multi-frequency driving, and route to quasiperiodicity

Experiments by Gommers et al. (2006, 2007) investigated the transition from periodic to quasiperiodic driving, and examined how the symmetry analysis is modified in this transition. In these experiments, a multifrequency driving was used, as obtained by combining signals at three different frequencies: ω_1, $2\omega_1$ and ω_2. For ω_2/ω_1 irrational the driving is quasiperiodic. Clearly, in a real experiment ω_2/ω_1 is always a rational number, which can be written as $\omega_2/\omega_1 = p/q$, with p, q two coprime positive integers. However, as the duration of the experiment is finite, by choosing p and q sufficiently large it is possible to obtain a driving which is effectively quasiperiodic on the time scale of the experiment. Different forms of multifrequency driving were examined in the experimental realizations, each probing a different symmetry.

The first form of driving examined by Gommers et al. (2006, 2007) consisted of the sum of three harmonics:

$$F(t) = A\cos(\omega_1 t) + B\cos(2\omega_1 t + \phi) + C\cos(\omega_2 t + \delta)\ . \tag{32}$$

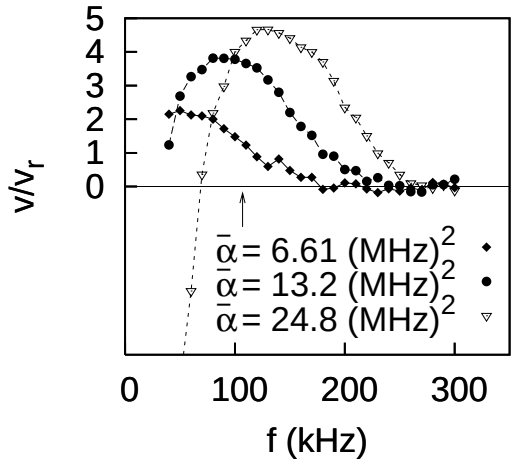

Fig. 10. Experimental results for the average atomic velocity as a function of the driving frequency $f = \omega/(2\pi)$, for different amplitudes of the driving force. As from Eqs. (30,31), for each data set the force is kept constant, while scanning the driving frequency, by varying the amplitude α_0 of the phase modulation according to $\alpha_0 = \bar{\alpha}/f^2$. The optical potential constant for all measurements corresponds to a vibrational frequency $\omega_v/(2\pi) = 170$ kHz. The driving frequency satisfying the condition $2\omega = \omega_v$ is indicated by an arrow. The values for the velocity are expressed in terms of the recoil velocity v_r, equal to 3.52 mm/s for the Cs D_2 line. The relative weight of the 2ω term of the modulation (see Eq. 30) is $\alpha_2 = 1$ for all data sets. The lines are guides for the eye. [Reprinted figure with permission from Gommers et al. (2005a). Copyright 2005 of the American Physical Society.]

In the analysis, the effects of dissipation can be neglected, as we know that it results in an additional phase shift. Consider first the case of periodic driving, with ω_2/ω_1 rational. For biharmonic driving, i.e. $C = 0$ in Eq. (32), the shift symmetry is broken for any value of ϕ, while the time-reversal symmetry is preserved for $\phi = n\pi$, with n integer. A current of the form $I \sim \sin\phi$ is obtained as a result. Consider now the effect of the third harmonic, i.e. $C \neq 0$ in Eq. (32. For a phase $\delta = 0$ of the ω_2 harmonic, this additional driving is invariant under time reversal, and therefore the total driving is still invariant under time-reversal for $\phi = n\pi$. Instead, for $\delta \neq 0$ the symmetry under time-reversal is broken and directed transport is allowed also for $\phi = n\pi$. In other words, for $\delta \neq 0$ the third driving leads to an additional phase shift of the current as a function of ϕ. The magnitude of such a shift depends on the phase δ. Taking dissipation also into account, it follows that the current will show the dependence $I \sim \sin(\phi - \phi_0)$ where ϕ_0 includes the phase shift produced by dissipation and the phase shift produced by the harmonic at frequency ω_2.

We now turn to the case of a quasiperiodic driving, as obtained in the case of irrational ω_2/ω_1. As discussed in Sec. 3.3 the symmetry analysis for the periodic driving can be generalized to the quasiperiodic case by treating the phases $\Psi_1 = \omega_1 t$ and $\Psi_2 = \omega_2 t$ as independent variables. We notice that the driving considered here, Eq. (32), is invariant under the transformation

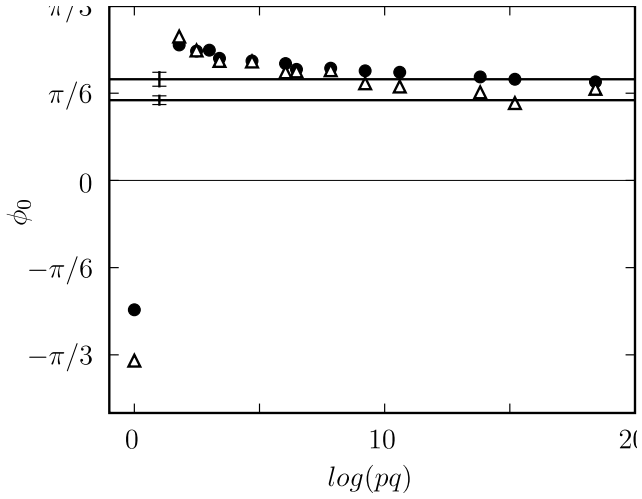

Fig. 11. Experimental results for the phase shift ϕ_0 as a function of pq which characterize the degree of periodicity of the driving. The two data sets, represented by open triangles and closed circles, correspond to different amplitudes of the driving. The two horizontal lines indicate the phase shift ϕ_0 for biharmonic drive, i.e., in the absence of the driving at frequency ω_2. [Reprinted figure with permission from Gommers et al. (2006). Copyright 2006 of the American Physical Society.]

$\Psi_2 \to -\Psi_2 + \chi_2$ for any δ, as δ can be reabsorbed in χ_2. Therefore the invariance under the transformation $\tilde{S}_2$ is entirely determined by the invariance of F under the transformation $\Psi_1 \to -\Psi_1 + \chi_1$; i.e., we recover the results for biharmonic driving: $\tilde{S}_2$ is a symmetry, and therefore directed motion is forbidden, for $\phi = n\pi$. Hence, in the quasiperiodic limit, the third harmonic at frequency ω_2 is not relevant for the symmetry of the system, which is entirely determined by the biharmonic term at frequency ω_1, $2\omega_1$.

In the experiment by Gommers et al. (2006), the transition to quasiperiodicity was investigated by studying the atomic current as a function of ϕ for $\omega_2/\omega_1 = p/q$ with p and q coprimes. By increasing p and q the driving can be made more and more quasiperiodic on the finite duration of the experiment, with the quantity pq a possible measure of the degree of quasiperiodicity. To verify the predictions of the symmetry analysis, the average atomic current was measured as a function of ϕ, for different choices of p and q. The data were fitted with the function $v = v_{max} \sin(\phi - \phi_0)$. The resulting value for the phase shift ϕ_0 is plotted in Fig. 11 as a function of pq.

For small values of the product pq, i.e., for periodic driving, the harmonic at frequency ω_2 leads to a shift which strongly depends on the actual value of pq. For larger values of pq, i.e., approaching quasiperiodicity, the phase shift ϕ_0 tends to a constant value. Such a value was found to be independent of δ, and coincides with the phase shift ϕ_0 measured in the case of pure biharmonic driving (horizontal lines in Fig. 11), which is determined by the finite damping of the atomic motion. The experimental results of Fig. 11 prove that,

in agreement with the symmetry analysis, in the quasiperiodic limit the only relevant symmetries are those determined by the periodic biharmonic driving and by dissipation. For a driving of a form Eq. 32, quasiperiodicity therefore restores the symmetries which hold in the absence of the additional driving which produced quasiperiodicity.

A different form of multi-frequency driving was also examined by Gommers et al. (2006). The driving force was obtained by multiplying the bi-harmonic driving at frequencies ω_1, $2\omega_1$ with the driving at frequency ω_2. This was done by applying to one of the lattice beams a frequency modulation of the form

$$\dot{\alpha}(t) = \alpha_0 \sin(\omega_2 t + \delta) \left[\sin(\omega_1 t) + \frac{\alpha_2}{4} \sin(2\omega_1 t)\right] \tag{33}$$

which results into a force

$$\begin{aligned} F(t) = -\frac{M\alpha_0}{k} \Big\{ & \omega_2 \cos(\omega_2 t + \delta) \left[\sin(\omega_1 t) + \frac{\alpha_2}{4} \sin(2\omega_1 t)\right] \\ & + \omega_1 \sin(\omega_2 t + \delta) \left[\cos(\omega_1 t) + \frac{\alpha_2}{2} \cos(2\omega_1 t\right] \Big\} \end{aligned} \tag{34}$$

It was shown that in this case quasiperiodicity results in the total suppression of transport.

Consider first the case of periodic driving. We indicate, as before, $\omega_2 = (p/q)\omega_1$. The period T of $F(t)$ is then $T = qT_1 = pT_2$, with $T_i = 2\pi/\omega_i$ $(i = 1, 2)$. Under the transformation $t \to t + T/2$ we have: $\omega_1 t \to \omega_1 t + q\pi$, $\omega_2 t \to \omega_2 t + p\pi$. By replacing these transformations in $F(t)$ it is straighforward to see that $F(t)$ satisfies the shift symmetry $F(t) = -F(t + T/2)$ if q is even, and p is odd. In this case directed transport is forbidden. If instead this condition is not satisfied, i.e. if q is odd, directed transport is not forbidden. In this case directed transport is controlled by the $\hat{S}_2$ symmetry which is realized, in the dissipationless limit, if the driving $F(t)$ is symmetric under time-reversal. The symmetry under time-reversal depends entirely on the phase δ of the driving at frequency ω_2: for $q\delta = (n+1/2)\pi$, with n integer, the driving is symmetric. Otherwise, the symmetry under time-reversal is broken. The current is expected to show a sinusoidal dependence on $q\delta - \pi/2$, and dissipation will account for an additional shift.

In the experiment, the average atomic velocity was measured as a function of δ for different values of the driving frequency $\omega_2 = (p/q)\omega_1$,with p, q co-primes. By fitting the data with $v = v_{max} \sin(q\delta - \delta_0)$, the maximum velocity v_{max} was determined as a function of ω_2. The results of Gommers et al. (2006) , shown in Fig. 12, demonstrate the relationship between symmetry and transport, valid in the periodic case, discussed above. In fact, a current was observed

only for values of the ratio of driving frequencies $\omega_2/\omega_1 = p/q$ with q odd, which is precisely the requirement for the shift symmetry to be broken.

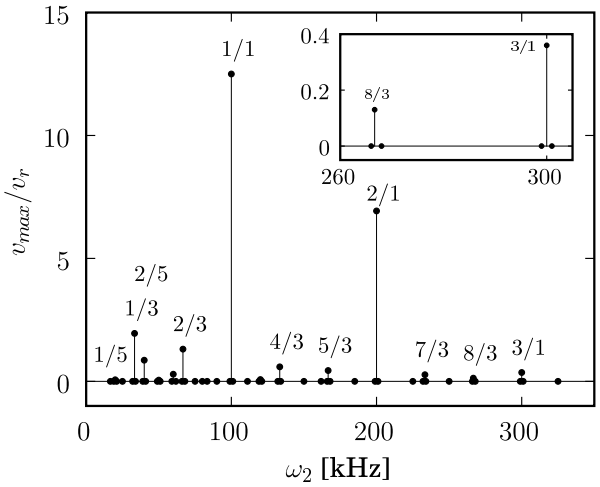

Fig. 12. Maximum average velocity as a function of the driving frequency ω_2. The data corresponding to a nonzero velocity are labelled by $p/q = \omega_2/\omega_1$. The inset magnifies a portion of the plot.[Reprinted figure with permission from Gommers et al. (2006). Copyright 2006 of the American Physical Society.]

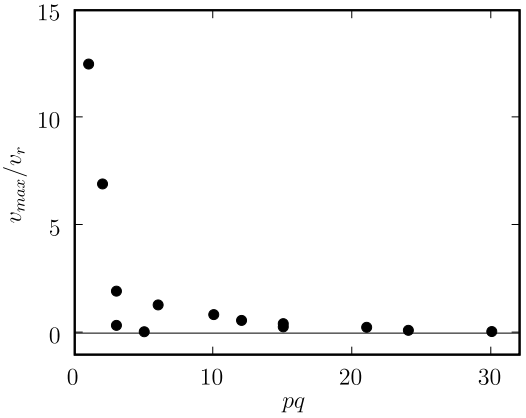

Fig. 13. Maximum average velocity as a function of pq, where p and q are the co-primes defined by the ratio of the driving frequencies: $p/q = \omega_2/\omega_1$. [Reprinted figure with permission from Gommers et al. (2006). Copyright 2006 of the American Physical Society.]

Consider now the case of quasiperiodic driving. To analyze this case, we introduce the two variables $\psi_1 = \omega_1 t$ and $\psi_2 = \omega_2 t$, to be treated as independent, and consider the generalized symmetries $\tilde{S}_1$, $\tilde{S}_2$. It is immediate to verify that F changes sign under the transformation $\psi_2 \to \psi_2 + \pi$, i.e. F is shift symmetric with respect to ψ_2. It follows that the system is invariant under the generalized symmetry $\tilde{S}_1$. Directed transport is therefore forbidden. In order to study the

transition to quasiperiodicity, the data of Fig. 12 were re-arranged as a function of pq which characterizes the quasiperiodic character of the driving on the finite duration of the experiment. The results are shown in Fig. 13. It appears that for large pq values the amplitude of the atomic current decreases to zero. This demonstrates that directed transport is destroyed in the quasiperiodic limit, as a results of the restoration of the shift symmetry of the driving.

4.5 Gating ratchet

As discussed in Sec. 3.4, in a gating ratchet particles experience an amplitude-modulated potential which is spatially symmetric. A zero-average and time-symmetric ac force is also applied. A current can be generated following a gating effect, with the lowering of the potential barriers synchronized with the motion produced by the additive force.

A gating ratchet for cold atoms was demonstrated experimentally by Gommers et al. (2008). The ratchet was realized with cold rubidium atoms in a driven 1D dissipative optical lattice. A single-harmonic periodic modulation of the potential depth was applied, together with a single harmonic rocking force. As in Sec. 3.4, the frequencies of the multiplicative (potential modulation) and additive (rocking force) drivings are denoted with ω_1 and ω_2, respectively, with the relative phase indicated by ϕ.

The results of Gommers et al. (2008) are reported in Fig. 14 and 15. In Fig. 14 the average atomic velocity is reported as a function of the phase offset ϕ. Different data sets were taken for different values of the ratio ω_2/ω_1. Figure 15 reports the corresponding current amplitude.

The experimental results of Figs. 14 and 15 constitute the experimental demonstration of a gating ratchet for cold atoms. The presence of both a single-harmonic additive driving and a single-harmonic multiplicative driving allows the breaking of the symmetries of the system, and a current is generated as a result.

The observations of Gommers et al. (2008) are in agreement with the symmetry analysis of Sec. 3.4. In fact, the analysis of the data for the different values of the driving frequencies ratio $\omega_2/\omega_1 = p/q$ shows that a current is generated only for q odd, as also evidenced in Fig. 15, and in this case the average atomic velocity exhibits a dependence on the phase ϕ of the form $v = v_{\max} \sin(q\phi + \phi_0)$.

As already pointed out in Sec. 3.4, there is an important difference between the gating ratchet realized by Gommers et al. (2008) and the previously demonstrated rocking ratchet with additive bi-harmonic driving (Schiavoni et al.,

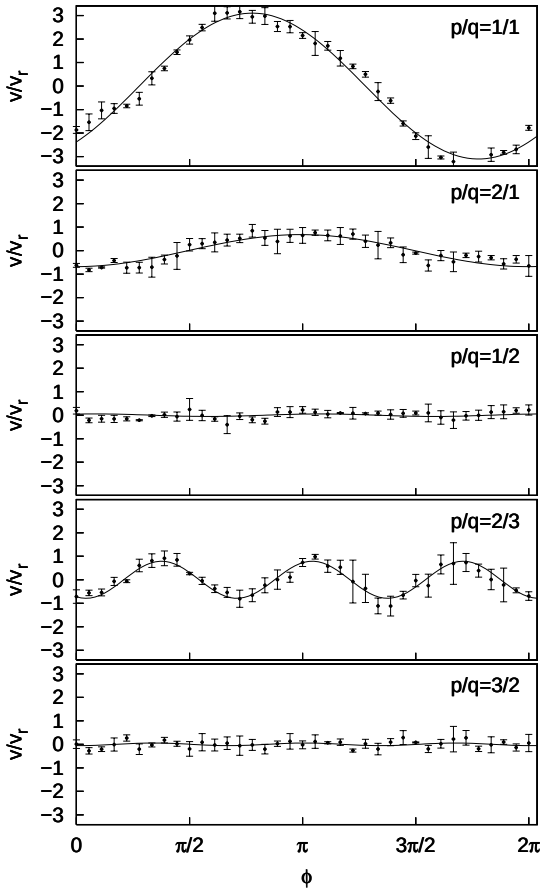

Fig. 14. Experimental results for a gating ratchet for cold atoms. The average atomic velocity is reported as a function of the phase offset ϕ between multiplicative and additive drivings. The atomic velocity is expressed in terms of the recoil velocity v_r, which for ^{87}Rb is equal to 5.9 mm/s. Different data sets correspond to different values of the frequency ω_2 of the additive (rocking) force. The frequency of the multiplicative driving is the same for all data sets, and it is equal to 150 kHz. The data sets are labelled by the ratio $p/q = \omega_2/\omega_1$. The lines are the best fits of the data with the function $v = v_{\max} \sin(q\phi + \phi_0)$. [Reprinted figure with permission from Gommers et al. (2008). Copyright 2008 of the American Physical Society.]

2003). In the rocking ratchet the underlying mechanism is harmonic mixing (Marchesoni, 1986), while the gating ratchet relies on a gating effect, with the lowering of the potential barriers synchronized with the motion produced by the additive force. This important difference is also manifest in the different conditions for the generation of a current. For example, in the gating ratchet a large current can be obtained when the two driving frequencies are equal, while the rocking ratchet requires harmonic mixing of two different frequencies.

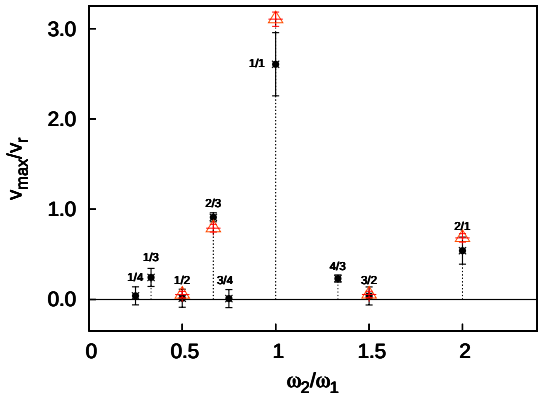

Fig. 15. Experimental results for the atomic current amplitude as a function of the frequency ratio ω_2/ω_1, as obtained by fitting data as those in Fig. 14 with the function $v = v_{\max} \sin(q\phi + \phi_0)$. The triangles represent the fit of the data of Fig. 14, the circles the fit of the data taken during a different measurement session. [Reprinted figure with permission from Gommers et al. (2008). Copyright 2008 of the American Physical Society.]

5 Outlook

This article reviewed recent experimental realization of ac driven ratchets with cold atoms in driven optical lattices.

Such a system allowed to realize experimentally rocking and gating ratchets, and to precisely investigate the relationship between symmetry and transport in these ratchets, both for the case of periodic and quasiperiodic driving.

The extreme tunability of optical lattices offers an unique possibility to investigate further the ratchet effect. For example, 2D and 3D optical lattices can be used to investigate complex multi-dimensional rectification mechanism (Denisov et al., 2008).

Disordered potentials and/or time-forces may be exploited to study the role of disorder in the transport in a ratchet device (Harms and Lipowsky, 1997; Marchesoni, 1997). Cold atoms in optical lattices may also allow for the realization of a quantum ratchet (Reimann et al., 1997), where the transport is produced by the interplay between tunneling and dissipation. Finally, the use of a Bose-Einstein condensate could allow to model the ratchet effect for vortices. By using multi-dimensional ratchet set-ups, as those proposed by Denisov et al. (2008), it should be possible to create vorticity in a controlled way. The very same ratchet set-up could then allow to control the vortex motion. This would constitute a clean model system for superconductor physics.

References

Ajdari, A. and Prost, J. (1992). *C.R. Acad. Sci. Paris* **315**, 1635.

Adjari, A., Mukamel, D., Peliti, L., and Prost, J. (1994). *J. Phys. I (France)* **4**, 1551.

Bartussek, R., Hänggi, P., and Kissner, J.G. (1994). *Europhys. Lett.* **28**, 459.

Brown M. and Renzoni F. (2008). *Phys. Rev. A* **77**, 033405.

Borromeo M., and Marchesoni, F. (2005). *Chaos* **15**, 026110.

Borromeo M., Giusepponi S., and Marchesoni F. (2006). *Phys. Rev. E* **74**, 031121.

Carminati, F.R., Schiavoni, M., Sanchez-Palencia, L., Renzoni, F., and Grynberg, G., (2001). *Eur. Phys. J. D* **17**, 249.

Chialvo, D.R. and Millonas M.M., (1996). *Phys. Lett. A* **209**, 26.

Cohen-Tannoudji, C., Dupont-Roc, J., Grynberg, G., (1998). *Atom-Photon Interactions*, Wiley.

Dalibard J. and Cohen-Tannoudji C., (1989). *J. Opt. Soc. Am.* **B6**, 2023.

Denisov S., Zolotaryuk Y., Flach S., and Yevtushenko O.(2008). *Phys. Rev. Lett.* **100**, 224102.

Devoret M.H., Martinis J.M., Esteve D., and Clarke J. (1984). *Phys. Rev. Lett.* **53**, 1260.

Devoret M.H., Esteve D., Martinis J.M., Cleland A., and Clarke J. (1987). *Phys. Rev. B* **36**, 58.

Doering, C.R., Horsthemke, W., and Riordan J. (1994). *Phys. Rev. Lett.* **72**, 2984.

Dykman M.I., Rabitz H., Smelyanskiy V.N., and Vugmeister B.E. (1997). *Phys. Rev. Lett.* **79**, 1178.

Dykman, M.I., Golding B., McCann L.I., Smelyanskiy V.N., Luchinsky D.G., Mannella R., McClintock P.V.E. (2001). *Chaos* **1**, 587.

Feynman R.P., Leighton R.B., and Sands M. (1963). *The Feynman Lectures on Physics* (Addison Wesley, Reading, MA), Vol. 1, Chap. 46.

Flach S., Yevtushenko O. and Zolotaryuk Y. (2000). *Phys. Rev. Lett.* **84**, 2358.

Flach S. and Denisov S. (2004) *Acta Phys. Pol.* **B35**, 1437.

Goychuk, I. and Hänggi, P. (1998). *Europhys. Lett.* **43**, 503.

Gommers R., Douglas P., Bergamini S., Goonasekera M., Jones P.H. and Renzoni F. (2005). *Phys. Rev. Lett.* **94**, 143001.

Gommers R., Bergamini S., and Renzoni F. (2005). *Phys. Rev. Lett.* **95**, 073003.

Gommers R., Denisov S. and Renzoni F. (2006). *Phys. Rev. Lett.* **96**, 240604.

Gommers R., Brown M., and Renzoni F. (2007). *Phys. Rev. A* **75**, 053406.

Gommers R., Lebedev V., Brown M., and Renzoni F. (2008). *Phys. Rev. Lett.* **100** 040603.

Grynberg G. and Mennerat-Robilliard C. (2001). *Phys. Rep.* **355**, 335.

Hagman, H., Dion C.M. , Sjolund, P., Petra, S.J.H., Kastberg, A. (2008). *Europh. Lett.* **81**, 33001.

Harms T. and Lipowsky R. (1997). *Phys. Rev. Lett.* **79**, 2895.

Jones P.H., Goonasekera M., and Renzoni F. (2004). *Phys. Rev. Lett.* **93**, 073904.
Luchinsky D.G., Greenall M.J., McClintock P.V.E. (2000). *Phys. Lett. A* **273**, 316.
Luczka, J., Bartussek, R. and Hänggi, P. (1995). *Europhys. Lett.* **31**, 431.
Marchesoni F. (1986). *Phys. Lett. A* **119**, 221.
Marchesoni F. (1997) *Phys. Rev. E* **56**, 2492.
Marchesoni F. and Hänggi P. (2009). *Rev. Mod. Phys.* in press.
Magnasco, M.O. (1993). *Phys. Rev. Lett.* **71**, 1477.
Mahato, M.C. and Jayannavar, A.M. (1995). *Phys. Lett. A* **209**, 21.
Mennerat-Robilliard, C., Lucas, D., Guibal, S., Tabosa, J., Jurczak, C., Courtois, J.-Y., and Grynberg, G. (1999). *Phys. Rev. Lett.* **82**, 851.
Neumann E. and Pikovsky A (2002). *Eur. Phys. J. B* **26**, 219.
Raithel, G., Birkl, G., Kastberg, A., Phillips, W.D., and Rolston, S.L. (1997). *Phys. Rev. Lett.* **78**, 630.
Reimann P. (2001). *Phys. Rev. Lett.* **86**, 4992.
Reimann P. (2002). *Phys. Rep.* **361**, 57.
Reimann P., Grifoni M., Hanggi P. (1997). *Phys. Rev. Lett.* **79**, 10.
Renzoni F. (2005). *Contemp. Phys.* **46**, 161.
Rousselet, J., Salome, L., Ajdari, A., and Prost, J., (1994). *Nature* **370**, 446.
Savel'ev S., Marchesoni F., Hänggi P., and Nori F. (2004). *Europhys. Lett.* **67**, 179.
Sanchez-Palencia, L., Schiavoni, M., Carminati, F.-R., Renzoni, F., and Grynberg, G. (2003). *J. Opt. Soc. Am. B* **20**, 925.
Schiavoni M., Sanchez-Palencia L., Renzoni F. and Grynberg G. (2003) *Phys. Rev. Lett.* **90**, 094101.
Sjolund P., Petra S.J.H., Dion C.M., Jonsell S., Nylen M., Sanchez-Palencia L., Kastberg A. (2006). *Phys. Rev. Lett.* **96**, 190602.
Sjolund P., Petra S.J.H., Dion C.M., Hagman H., Jonsell S., Kastberg A. (2007). *Eur. Phys. J. D* **44**, 381.
Soskin S.M., Mannella R., and McClintock P.V.E. (2003). *Phys. Rep.* **373**, 247.
Yevtushenko O., Flach S., Zolotaryuk Y. and Ovchinnikov A.A. (2001). *Europhys. Lett.* **54**, 141.